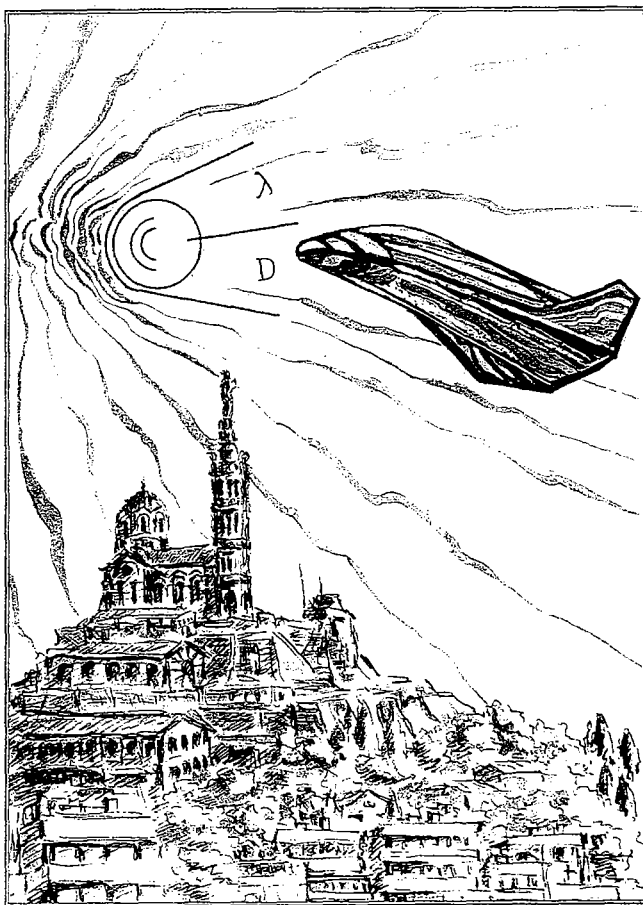# RAREFIED GAS DYNAMICS

Volume 1

EDITORS
R. BRUN, R. CAMPARGUE, R. GATIGNOL, J.-C. LENGRAND

CÉPADUÈS ÉDITIONS

Non-Newtonian Shear Viscosity in a Dense System of Hard Disks

J.M. Montanero[1], A. Santos[2]
[1] Departamento de Electrónica e Ingeniería Electromecánica,
Universidad de Extremadura, E-06071 Badajoz, Spain
[2] Departamento de Física,
Universidad de Extremadura, E-06071 Badajoz, Spain

1 Introduction

Kinetic theory can be viewed as an intermediate step between a detailed microscopic analysis of a many-body system and the corresponding phenomenological macroscopic description. In kinetic theory the main objective is to derive and solve the kinetic equation for the one-particle distribution function, thus obtaining information about the system properties. In the context of dilute gases, the Boltzmann equation (BE) [1] provides the adequate framework for studying states arbitrarily far from equilibrium. Exact solutions to this equation are rare, but a great deal of information can be obtained from simplified kinetic models [2] or from simulation Monte Carlo methods [3]. On the other hand, the assumptions implicit in the BE are only physically justified in the low-density limit. As the density increases, structural effects become important, potential contributions to the fluxes dominate, and the BE is no longer adequate. There is no general kinetic equation valid for finite densities. A singular exception, however, is the idealized system of hard spheres of diameter σ, for which Enskog proposed a semi-phenomenological equation [1] by introducing two crucial changes in the Boltzmann collision integral: (a) the centers of two colliding particles are separated by a distance equal to σ; (b) the collision frequency is increased by a factor that accounts for the spatial correlation between the two colliding molecules. Although the Enskog equation (EE) also ignores the correlations in the velocities before collision (*stosszahlansatz*), it leads to transport coefficients that are in good agreement with experimental and simulation values for a wide range of densities. In addition, the revised Enskog theory (RET) [4] is asymptotically exact at short times and therefore has no limitations on density or space scale in that limit. Moreover, it admits both fluid and crystal equilibrium states as stationary solutions.

The mathematical complexity of the EE has hindered practical applications. As in the case of BE, two different approaches have been proposed to cope with this problem. First, a Monte Carlo algorithm has been introduced to solve numerically the EE [5], in the same spirit as the DSMC method of solving the BE [3]; second, a simple kinetic model that retains the main features of the EE has been constructed [6, 7]; it reduces in the low density limit to the simplest kinetic model of the BE, the Bhatnagar-Gross-Krook (BGK) model. Both approaches have demonstrated to succeed in capturing the essential properties of the EE and have great potential for a new understanding of nonequilibrium systems under conditions accessible previously only by molecular dynamics simulation.

Two-dimensional systems often serve as prototypes to investigate some physical properties also present in real systems. In particular, many of the peculiarities of a hard-sphere fluid in far from equilibrium states are expected to be present in a hard-disk system with a similar value of the packing fraction. Obviously, the calculations usually become easier from both theoretical and computational points of view. In this paper we calculate the rheological properties of a dense fluid of hard disks under shear far from equilibrium by using a kinetic model of the EE. The results are compared with Monte Carlo simulations. As happens in the three-dimensional case [7], the comparison shows an excellent agreement at all densities and shear rates considered.

2   The Enskog Equation for a Hard-Disk Fluid under Uniform Shear Flow

The uniform shear flow (USF) is one of the few inhomogeneous states for which exact results can be obtained far from equilibrium, and therefore is of great significance in providing insight for the type of phenomena that occur under extreme state conditions. Moreover, it has been studied extensively by molecular dynamics simulation to analyze rheological properties in simple atomic fluids. The macroscopic state is characterized by a constant density n, a uniform temperature T, and a linear flow field: $\mathbf{u}(\mathbf{r}) = \mathbf{a} \cdot \mathbf{r} = ay\hat{\mathbf{x}}$, where $\mathbf{a} = a\hat{\mathbf{x}}\hat{\mathbf{y}}$. The (constant) shear rate a is a single parameter that can be chosen to drive the system arbitrarily far from equilibrium. The shear produces viscous heating that is compensated by an external nonconservative force (thermostat), $\mathbf{F} = -m\alpha(a)\mathbf{V}$, where m is the mass of a particle, $\mathbf{V} = \mathbf{v} - \mathbf{u}$ is the peculiar velocity, and the thermostat parameter α is adjusted to assure that the temperature remains constant. At a microscopic level, the USF is characterized by a distribution function, $f(\mathbf{r}, \mathbf{v}, t) \rightarrow f(\mathbf{V}, t)$, that becomes uniform in the Lagrangian frame of reference. Under the above

conditions, the EE for $f(\mathbf{V}, t)$ becomes

$$\left(\frac{\partial}{\partial t} - aV_y \frac{\partial}{\partial V_x} - \alpha \frac{\partial}{\partial \mathbf{V}} \cdot \mathbf{V} \right) f = J_E[f] , \tag{1}$$

where $J_E[f]$ is the Enskog collision operator,

$$J_E[f] = \sigma \chi(n) \int d\mathbf{V}_1 \int d\hat{\sigma} \, \Theta(\hat{\sigma} \cdot \mathbf{g}) \, (\hat{\sigma} \cdot \mathbf{g})[f(\mathbf{V}', t) f(\mathbf{V}'_1, t) - f(\mathbf{V}, t) f(\mathbf{V}_1, t)] . \tag{2}$$

In the above expression σ is the disk diameter, $\chi(n)$ is the pair correlation function at contact for an equilibrium system with (uniform) density n, $\hat{\sigma}$ is a unit vector, $\Theta(x)$ is the Heaviside function, $\mathbf{g} = \mathbf{V} - \mathbf{V}_1 - \sigma \mathbf{a} \cdot \hat{\sigma}$, $\mathbf{V}' = \mathbf{V} - (\hat{\sigma} \cdot \mathbf{g})\hat{\sigma}$, and $\mathbf{V}'_1 = \mathbf{V}_1 + 2\sigma \mathbf{a} \cdot \hat{\sigma} + (\hat{\sigma} \cdot \mathbf{g})\hat{\sigma}$.

The most relevant transport quantity is the steady-state pressure tensor P, which measures shear and normal stresses. It has a kinetic part, P^k, and a collisional transfer part, P^c, that are functionals of f given by

$$\mathsf{P}^k = m \int d\mathbf{V} \, \mathbf{V}\mathbf{V} f(\mathbf{V}) , \tag{3}$$

$$\mathsf{P}^c = \frac{m\sigma^2 \chi}{2} \int d\mathbf{V} \int d\mathbf{V}_1 \int d\hat{\sigma} \, \hat{\sigma}\hat{\sigma} \, \Theta(\hat{\sigma} \cdot \mathbf{g})(\hat{\sigma} \cdot \mathbf{g})^2 f(\mathbf{V} + \sigma \mathbf{a} \cdot \hat{\sigma}) f(\mathbf{V}_1) . \tag{4}$$

Following the standard Chapman-Enskog method [1], the Navier-Stokes constitutive equations are derived and the Newtonian shear viscosity can be identified as [8]

$$\eta_{\mathrm{NS}}(n) = \frac{\eta_0}{\chi} \left(1 + \frac{\pi}{4} n^* \chi \right)^2 + \frac{1}{4\sigma} n^{*2} \chi (\pi m k_B T)^{1/2} , \tag{5}$$

where $\eta_0 = 1.022(mk_B T/\pi)^{1/2}/2\sigma$ is the Boltzmann viscosity, k_B is the Boltzmann constant, and $n^* = n\sigma^2$ is the reduced density. This Navier-Stokes shear viscosity is the zero shear rate limit ($a \rightarrow 0$) of a generalized transport coefficient $\eta(n, a) = -P_{xy}/a$. Other non-Newtonian effects are associated with the differences $P_{xx}(n, a) - p_0(n)$ and $P_{yy}(n, a) - p_0(n)$, where $p_0(n) = nk_B T(1 + \frac{\pi}{2} n^* \chi)$ is the equilibrium hydrostatic pressure.

3   The Kinetic Model

Very recently, a kinetic model has been derived by replacing the Enskog collision operator with a simpler form that, otherwise, retains the main qualitative features. The model has the same domain of applicability and preserves the same basic properties (such as local conservation laws and the exact equilibrium stationary state for both fluid and crystal phases) as the RET. For a detailed account of the kinetic model, we refer the reader to

Refs. [6, 7]. In the particular case of the USF, the kinetic model leads to the replacement

$$J_E[f] \to -\nu(f - f_\ell) - f_\ell \left[\frac{P_{xy}^c}{nk_BT} a \left(\frac{m}{2k_BT} V^2 - 1 \right) - \frac{2m}{k_BT} V_x V_y A_{xy} \right] , \quad (6)$$

where we have already considered the two-dimensional case. In Eq. (6) ν represents an effective collision frequency depending on the local density and temperature. Here, this parameter is chosen to assure that the low density shear viscosity is the same as that from the BE, $\nu = nk_BT\chi/\eta_0$. In addition, $f_\ell(\mathbf{V})$ is the local equilibrium distribution, P_{xy}^c is the xy-element of the collisional transfer pressure tensor, as obtained from Eq. (4), and A_{xy} is the collisional moment

$$A_{xy} = \frac{m}{2nk_BT} \int d\mathbf{V} V_x V_y J_E[f_\ell] = -\frac{\pi}{4} (k_BT/m)^{\frac{1}{2}} n\sigma\chi\bar{a} \left(1 + \frac{3}{8}\bar{a}^2 \right) , \quad (7)$$

where $\bar{a} \equiv \frac{1}{2}a\sigma(m/k_BT)^{1/2}$. Equation (1) together with the substitution (6) constitutes now the kinetic equation for the problem. Since the term P_{xy}^c is a functional of f, Eq. (1) [along with (6)] is still a highly nonlinear integro-differential equation.

In order to ease the notation, we choose units such that $\nu = 1$, $m = 1$, and $2k_BT/m = 1$, and define the dimensionless pressure tensor $\mathbf{P}^* \equiv \mathbf{P}/nk_BT$. In these units, $\sigma = (\sqrt{2\pi}/1.022)n^*\chi$. Conservation of energy gives the thermostat parameter $\alpha(a)$ in terms of $P_{xy}^*(a)$:

$$\alpha(a) = -\frac{a}{2} P_{xy}^*(a) . \quad (8)$$

Taking moments in both sides of the (stationary) kinetic equation, one can easily get the kinetic part of the pressure tensor:

$$P_{xx}^{k*} = 1 + \frac{a^2 - 2aA_{xy}}{(1+2\alpha)^2 + a^2} , \quad P_{xy}^{k*} = \frac{1+2\alpha}{(1+2\alpha)^2 + a^2}(2A_{xy} - a) . \quad (9)$$

In order to close the mathematical problem, we would need to express P_{xy}^{c*} in terms of α. In principle, this implies to perform the velocity integrals (4) with the formal solution to the kinetic equation. Instead, we obtain a reasonable estimate for P_{xy}^{c*} by using the first Sonine approximation

$$f \to f_\ell \left[1 + (V_x^2 - V_y^2)(P_{xx}^{k*} - 1) + 2V_x V_y P_{xy}^{k*} \right] . \quad (10)$$

With this approximation, the evaluation of $\mathbf{P}^{c*}$ is similar to that of A_{xy}. In particular,

$$\begin{aligned}
P_{xy}^{c*} &= -\frac{n^*\chi}{2} \int d\hat{\sigma} \; \hat{\sigma}_x \hat{\sigma}_y \left\{ (1 + 2\bar{a}^2\hat{\sigma}_x^2\hat{\sigma}_y^2) \; \mathrm{erf}(\bar{a}\hat{\sigma}_x\hat{\sigma}_y) - 2\hat{\sigma}_x\hat{\sigma}_y P_{xy}^{k*} \right. \\
&\quad \left. + \frac{\bar{a}\hat{\sigma}_x\hat{\sigma}_y}{4\sqrt{\pi}} e^{-\bar{a}^2\hat{\sigma}_x^2\hat{\sigma}_y^2} \left[8 - \left(2\hat{\sigma}_x^2 - 1\right)^2 \left(P_{xx}^{k*} - 1\right)^2 - 4\hat{\sigma}_x^2\hat{\sigma}_y^2 P_{xy}^{k*2} \right] \right\} .
\end{aligned}$$

$$\quad (11)$$

From Eqs. (8), (9) and (11) one gets a *closed* equation for α, whose numerical solution can be easily obtained for arbitrary shear rates and densities.

4   The ESMC Method

As discussed in the Introduction, a recent method has been developed for Monte Carlo simulation of the solution to the EE [5]. Previous results have demonstrated the utility of this Enskog simulation Monte Carlo (ESMC) method for studying far from equilibrium states in the regime of low and moderate densities. In these conditions, the ESMC method can be even more efficient, from a computational point of view, than hard-sphere molecular dynamics. In addition, the ESMC algorithm reduces to the well-known DSMC method [3] in the low density limit.

As applied to the USF, the method proceeds as follows. The one-particle distribution function $f(\mathbf{V})$ is represented by the peculiar velocities $\{\mathbf{V}_i\}$ of a sample of N "simulated" particles. These velocities are updated at integer times $t = \Delta t, 2\Delta t, 3\Delta t, \ldots$, where the time-step Δt is much smaller than the mean free time and the inverse shear rate. This is done in two stages: free streaming and collisions. The free streaming stage consists of making

$$\mathbf{V}_i \to e^{-\alpha\Delta t}(\mathbf{V}_i - \mathbf{a} \cdot \mathbf{V}_i\Delta t) , \quad (12)$$

where the thermostat parameter α is adjusted to assure that the temperature, which is computed as $T = (m/Nk_B)\sum_i V_i^2$, remains constant. In the collision stage, a sample of $\frac{1}{2}N\tilde{w}$ pairs are chosen at random with equiprobability, where $\tilde{w}$ is an upper bound estimate of the probability that a particle collides in the time interval between t and $t + \Delta t$. For each pair ij belonging to this sample, the following steps are taken: (1) a given direction $\hat{\sigma}_{ij}$ is chosen at random with equiprobability; (2) the collision between particles i and j is accepted with a probability equal to the ratio $w_{ij}/\tilde{w}$, where $w_{ij} = 2\pi\sigma\chi n\Delta t\Theta(\hat{\sigma}_{ij} \cdot \mathbf{g}_{ij})(\hat{\sigma}_{ij} \cdot \mathbf{g}_{ij})$ and $\mathbf{g}_{ij} = \mathbf{V}_i - \mathbf{V}_j - \sigma\mathbf{a} \cdot \hat{\sigma}_{ij}$; and (3) if the collision is accepted, post-collision velocities are assigned to both particles:

$$\mathbf{V}_i \to \mathbf{V}_i - \hat{\sigma}_{ij}(\hat{\sigma}_{ij} \cdot \mathbf{g}_{ij}) , \quad \mathbf{V}_j \to \mathbf{V}_j + \hat{\sigma}_{ij}(\hat{\sigma}_{ij} \cdot \mathbf{g}_{ij}) . \quad (13)$$

In the case that in one of the collisions $w_{ij} > \tilde{w}$, the estimate of $\tilde{w}$ is updated as $\tilde{w} = w_{ij}$. In the course of the simulations, the kinetic and collisional transfer contributions to the pressure tensor are evaluated. They are given as the computational analogs of Eqs. (3) and (4), i.e.

$$\mathbf{P}^k = \frac{mn}{N} \sum_{i=1}^{N} \mathbf{V}_i \mathbf{V}_i , \quad (14)$$
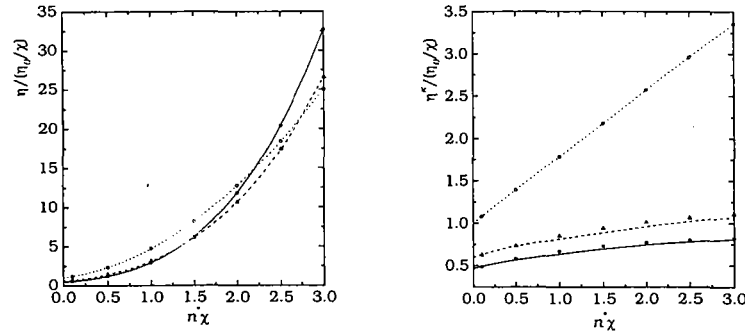
Figure 1: Plot of the normalized shear viscosity $\eta/(\eta_0/\chi)$ and its kinetic part $\eta^k/(\eta_0/\chi)$ for $a = 0$ $(\cdots)$, $a = 0.7$ $(--)$, and $a = 1$ $(—)$. Lines are from the kinetic model; symbols are from Monte Carlo simulations of the EE.

$$\mathsf{P}^c = \frac{mn}{N} \frac{\sigma}{\Delta t} \sum_{ij}^{\dagger} (\widehat{\sigma}_{ij} \cdot \mathbf{g}_{ij}) \widehat{\sigma}_{ij} \widehat{\sigma}_{ij} , \qquad (15)$$

where the dagger means that the summation is restricted to the accepted collisions. Once the steady state is reached, the above quantities are averaged over time to improve the statistics.

5   Results and Discussion

Our objective has been to obtain the pressure tensor P as a function of the density and the shear rate by means of the kinetic model, as well as by performing Monte Carlo simulations of the EE.

Figure 1 shows a comparison of the (normalized) non-Newtonian shear viscosity $\eta = -P_{xy}/a$ as a function of the density parameter $n^*\chi$ for three different values of the shear rate. The corresponding kinetic part is also shown in the right side of the figure. In all the figures presented in this paper, the error bars are smaller than the sizes of the symbols and are not drawn. The good agreement indicates that both the kinetic and collisional transfer contributions are accurately given by the model. The dotted lines correspond to the Navier-Stokes shear viscosity, Eq. (5), so that the solid and the dashed lines represent non-Newtonian effects. It is quite apparent that these effects are much more important at finite density than at zero density. It is worthwhile noticing that the shear viscosity presents, in general, a non monotonic behavior as the shear rate increases. More precisely, a transition from shear thinning, $\eta(n,a) < \eta_{NS}(n)$, to shear thickening, $\eta(n,a) > \eta_{NS}(n)$, takes place when the shear rate is larger than a critical
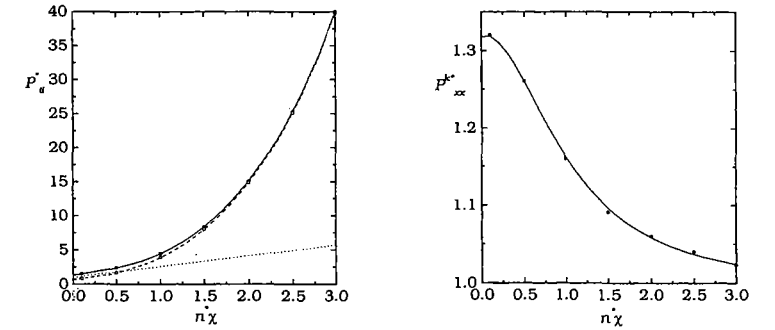
Figure 2: Plot of P_{xx}^* $(—)$, P_{yy}^* $(--)$ and p_0^* $(\cdots)$ (left side), and the kinetic part P_{xx}^{k*} (right side), for $a = 1$. Lines are from the kinetic model; symbols are from Monte Carlo simulations of the EE.

value $a_c(n)$ that decreases as the density increases. In particular, $a_c = 1.0$ at $n^*\chi \simeq 2.2$, while $a_c = 0.7$ at $n^*\chi \simeq 2.7$. This transition has been recently predicted for a hard-sphere fluid from an analysis of the kinetic model in the limit of small shear rates and confirmed by the ESMC method [7]. This is an interesting effect not observed for the kinetic part.

Figure 2 shows the (dimensionless) normal stresses P_{xx}^* and P_{yy}^* as functions of the density for the shear rate $a = 1$. The dotted line represents the equilibrium hydrostatic pressure $p_0^* = 1 + \frac{\pi}{2}n^*\chi$ of a hard-disk fluid. Again, the numerical solution of the model shows an excellent agreement for the wide range of densities considered. At high densities the collisional part of the pressure tensor dominates and both diagonal elements P_{xx}^* and P_{yy}^* tend to coincide. In addition, viscometric effects become evident by observing the increase of the nonequilibrium "hydrostatic pressure" $p^* = \frac{1}{2}\text{tr}\mathsf{P}^*$ with respect to its equilibrium value p_0^*, a phenomenon usually referred to as "shear dilatancy". The kinetic contribution P_{xx}^{k*} is also plotted in Fig. 2. Note that the yy-element can be derived from the consistency condition $P_{xx}^{k*} + P_{yy}^{k*} = 2$. We observe that again a good accuracy of the model predictions holds for these quantities.

In this work we have presented results obtained from both a kinetic model [6] and a simulation Monte Carlo method of the EE [5] for a hard-disk system under shear, arbitrarily far from equilibrium. Although the EE is not expected to be accurate for very large densities, we have also considered those densities in order to check the kinetic model predictions. Comparison between the results obtained from the ESMC method and from the numerical solution of the model shows an excellent agreement, so that we can conclude that the kinetic model gives a good description of the rheological

properties throughout the whole shear rate-density plane. In particular, we have analyzed non-Newtonian effects beyond Navier-Stokes order by computing the elements of the pressure tensor. A transition from shear thinning to shear thickening is clearly shown by using both approaches.

References

[1] Chapman S. and Cowling T.G., *The Mathematical Theory of Non-Uniform Gases*, Cambridge University Press, 1970.

[2] Dufty J.W., *Kinetic theory of fluids far from equilibrium — Exact results*, in *Lectures in Thermodynamics and Statistical Mechanics*, López de Haro M. and Varea C., eds., World Scientific, pp.166–181, 1990.

[3] Bird G.A., *Molecular Gas Dynamics and the Direct Simulation of Gas Flows*, Clarendon Press, 1994.

[4] van Beijeren H. and Ernst M.H., *The modified Enskog equation*, Physica, Vol.68, pp.437–456, 1973.

[5] Montanero J.M. and Santos A., *Monte Carlo Simulation Method for the Enskog Equation*, Phys. Rev. E, Vol.54, No.1, pp.438–444, 1996; *Viscometric Effects in a Dense Hard-Sphere Fluid*, Physica A, Vol.240, Nos.1–2, pp.229–238, 1997. *Simulation of the Enskog Equation à la Bird*, Phys. Fluids, Vol.9, No.7, pp.2057–2060, 1997; Frezzotti, A., *A particle scheme for the numerical solution of the Enskog equation*, Phys. Fluids, Vol.9, No.5, pp.1329–1335.

[6] Dufty J.W., Santos A., and Brey J.J., *Practical Kinetic Model for Hard Sphere Dynamics*, Phys. Rev. Lett., Vol.77, No.7, pp.1270–1273, 1996; Dufty J.W., Brey J.J., and Santos A., *Kinetic models for hard sphere dynamics*, Physica A, Vol.240, Nos.1–2, pp.212–220, 1997.

[7] Santos A., Montanero J.M., Dufty J.W., and Brey J.J., *Kinetic Model for the hard-sphere fluid and solid*, Phys. Rev. E, Vol.57, No.2, pp.1644–1660, 1998.

[8] Gass D.M., *Enskog Theory for a Rigid Disk Fluid*, J. Chem. Phys., Vol.54, No.5, pp.1898–1902, 1971.